Supplement of Biogeosciences, 23, 1965–1985, 2026
https://doi.org/10.5194/bg-23-1965-2026-supplement
© Author(s) 2026. CC BY 4.0 License.

Biogeosciences Open Access EGU

Supplement of

Photochemistry of the sea-surface microlayer (SML) influenced by a phytoplankton bloom: a mesocosm study

Olenka Jibaja Valderrama et al.

Correspondence to: Hartmut Herrmann (herrmann@tropos.de)

The copyright of individual parts of the supplement might differ from the article licence.

S1 Ferrioxalate actinometry

The ferrioxalate actinometer is among the most widely used system due to its strong absorption in the UV-Vis spectrum. When exposed to light, Fe(III) oxalate complex photochemically decomposed to form Fe(II) oxalate complex, and this process can be quantified via complexation with 1,10-phenanthroline (Hatchard and Parker, 1956). The simplified reaction mechanisms for the photolysis of Fe(III) and the complexation of Fe(II) with 1,10 phenanthroline are:

$$Fe(III)(C_2O_4)_3^{3-} + h\nu \rightarrow Fe(II)(C_2O_4)_2^{2-} + CO_2 + CO_2^{\cdot-} \quad \text{(SR1)}$$

$$Fe(II) + 3\,phen \rightarrow Fe(II)(phen)_3 \quad \text{(SR2)}$$

The potassium ferrioxalate solution was placed inside the photoreactor and the first aliquot (2 mL) was extracted before the irradiation with the same solar simulator used for the ambient seawater samples. After that, the Xe lamp was turned on and light-exposed aliquots (2 mL each) were collected every 20 seconds for 2 minutes. The time was accurately controlled using a timer. All this process took place under continuous stirring. Right after extraction, all the collected aliquots were put together in amber glass bottles with the previously prepared mixtures of ultra-pure water, sodium acetate, 1,10-phenanthroline hydrochloride monohydrate (Fluka) and sulphuric acid (96 %, Merck) to form the complex. The total volume of the complex was 10 mL. The volumes of each solution of the mixture were chosen so the measured absorbance of the complex at 510 nm was below 1.0. The amber glass bottles were covered with aluminium foil and stored in a dark shelf for 40 minutes to complete the complexation. After that, the absorbance of each sample at 510 nm was measured in high performance 10 x 10 mm quartz glass cuvette (Hellma) with a UV/VIS spectrometer (PerkinElmer Instruments). Data was acquired using the Lambda 900 software. The absorbance of the complexes for each light-exposure time was calculated from the average of two values measured consecutively. The molar concentrations of the complexes ($c_{complex}$, mol L^{-1}) were calculated using the Lambert-Beer law:

$$A_{510\,nm} = \varepsilon_{510\,nm} \times l \times c_{complex} \quad \text{(S1)}$$

Where $A_{510\,nm}$ is the absorbance at 510 nm, $\varepsilon_{510\,nm}$ is the molar absorption coefficient of the complex at 510 nm (11100 L mol^{-1} cm^{-1}) (Goldstein and Rabani, 2008), l is the pathlength (1 cm). The molar concentration of Fe(II) produced in each sample ($c_{Fe(II)}$) was determined from the calculated molar concentrations of the complexes, the volume of actinometer extracted (2 mL), and the volume of complex prepared (10 mL). The wavelength-dependent photon fluxes (q_λ, moles of photons L^{-1} s^{-1}) were obtained from:

$$q_\lambda = \frac{\phi_\lambda \times c_{Fe(II)}}{t} \quad \text{(S2)}$$

Where ϕ_λ is the wavelength-dependent quantum yield for the formation of Fe(II), and t is light-exposure time (s). The quantum yield used for the estimations is the average of the quantum yields reported for the same concentrations of potassium ferrioxalate solutions (Hatchard and Parker, 1956; Wegner and Adamson, 1966; Demas et al., 1981; Lee and Seliger, 1964; Langford and Holubov, 1981), and for wavelengths relevant in the sea-surface (290 to 509 nm).

S2 Setup used for in situ EPR spectroscopy experiments

35

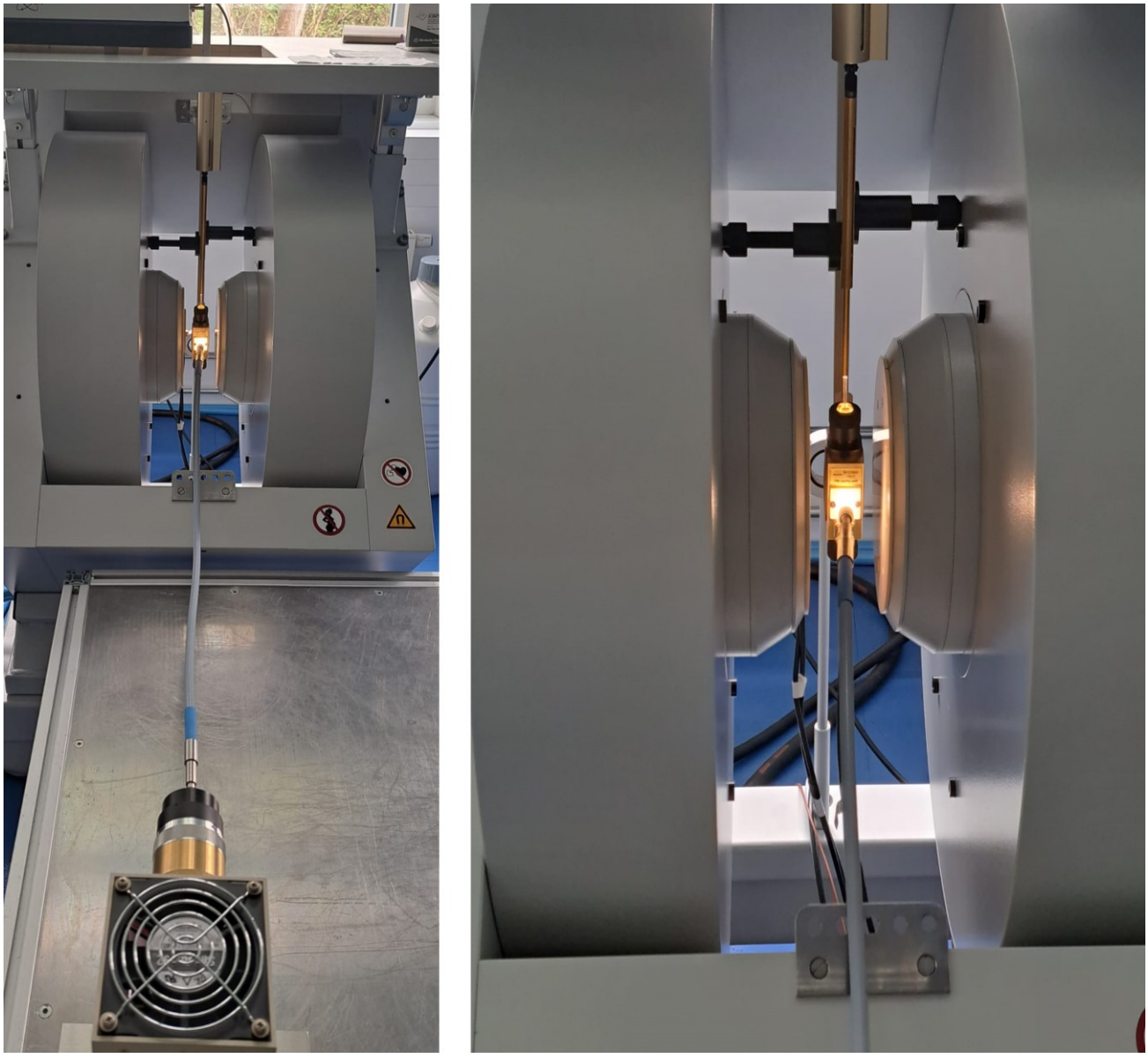

Figure S1: The setup used in the in situ EPR experiments.

S3 EPR control tests in the presence of Fe(II), Fe(III), Cu(I), and Cu(II) chloride salts

To attest to the participation of direct electron transfer between transition metal ions dominant in the SML and ULW samples, control experiments were performed in the presence of $FeCl_3$, $FeCl_2$, CuCl and $CuCl_2$. Chloride salts were chosen due to the prevalence of chloride in the samples. In situ EPR experiments were conducted in the presence of 500 nM of each individual salt and in mixtures between Fe and Cu salts. As can be seen in Figure S2, Cu had a big influence on the monitored rates of CM radical formation, with formation rates reaching 16 μM s^{-1}. Fe salts presented minor activity. Responses were corrected considering the photon-fluxes estimated for the PR (Photochemical reactor) as follows:

$$Corrected\ responses = Rate\ CM\ radical\ formation \times \frac{I_{PR}}{I_{EPR}} \quad \text{(S3)}$$

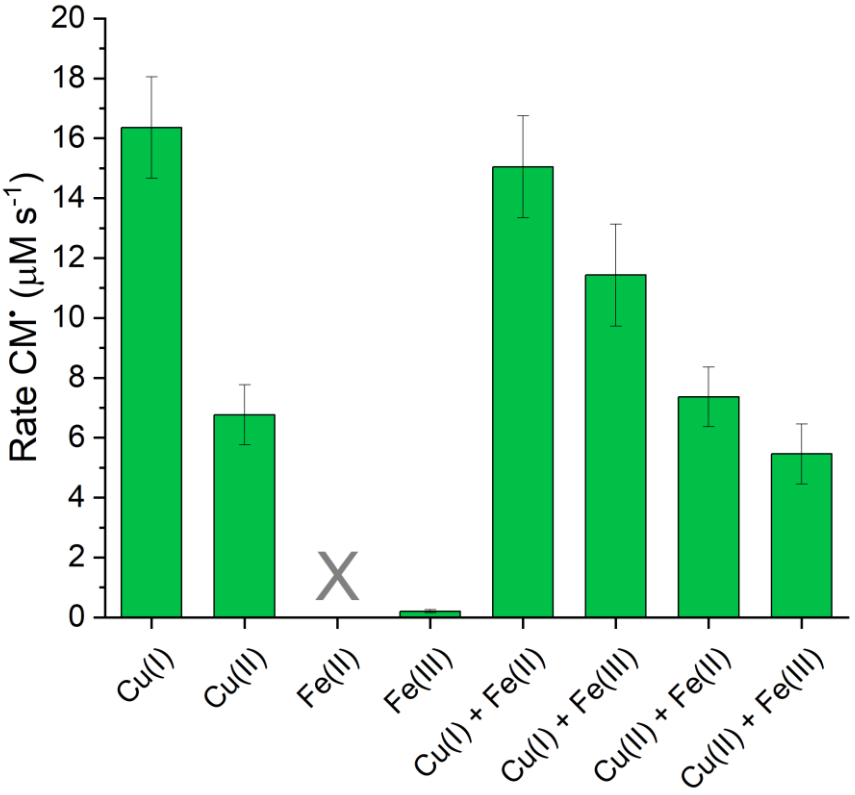

Figure S2: EPR control tests in the presence of Fe(II), Fe(III), Cu(I), and Cu(II) chloride salts.

S4 Concentrations of carbonyl compounds in the SML and ULW samples

Table S1: Concentrations of carbonyl compounds in nmol L^{-1} before, after 2.5 hours and after 5 hours of irradiation for samples collected on May 20th.

Compound	SML			ULW		
	Before irradiation	After 2.5 hours of irradiation	After 5 hours of irradiation	Before irradiation	After 2.5 hours of irradiation	After 5 hours of irradiation
Acetophenone	20	25	32	n.d.	1	6
Acrolein	0	0	539	n.d.	n.d.	n.d.
Benzaldehyde	4097	3872	3710	27	57	91
Biacetyl	1368	1285	1548	326	369	386
Butanal	16	111	270	79	128	173
Crotonaldehyde	n.d.	n.d.	n.d.	n.d.	n.d.	n.d.
Glyoxal	2138	2164	2620	945	995	1097
Heptanal	793	828	981	160	159	222
Hexanal	2806	2786	3171	572	580	771
Isovaleraldehyde	1381	1420	1490	197	221	276
Methacrolein	n.d.	n.d.	n.d.	n.d.	n.d.	n.d.
Methylglyoxal	1136	1179	1522	1635	1552	1650
MVK	1081	1246	1469	529	4734	482
Octanal	75	n.d.	18	57	8	111
Propanal	1457	1933	2606	1756	2053	2202
Trans-2-hexenal	53	47	7	12	20	18
Trans,trans-2,4-hexadienal	34	45	52	21	23	23

n.d.: Not detectable

Table S2: Concentrations of carbonyl compounds in nmol L^{-1} before, after 2.5 hours and after 5 hours of irradiation for samples collected on May 22nd.

Compound	SML			ULW		
	Before irradiation	After 2.5 hours of irradiation	After 5 hours of irradiation	Before irradiation	After 2.5 hours of irradiation	After 5 hours of irradiation
Acetophenone	40	39	48	n.a.		
Acrolein	2621	1982	1108			
Benzaldehyde	3626	3101	2802			
Biacetyl	2968	3132	3511			
Butanal	38	n.d.	n.d.			
Crotonaldehyde	1033	309	n.d.			
Glyoxal	2022	1952	1786			
Heptanal	1787	1596	2217			
Hexanal	13198	11600	12451			
Isovaleraldehyde	4174	2729	1638			
Methacrolein	8723	7974	7698			
Methylglyoxal	545	451	657			
MVK	12439	13835	14781			
Octanal	57	295	644			
Propanal	5099	3179	2293			
Trans-2-hexenal	154	190	275			
Trans,trans-2,4-hexadienal	67	62	63			

n.d.: Not detectable; n.a.: Not available

Table S3: Concentrations of carbonyl compounds in nmol L^{-1} before, after 2.5 hours and after 5 hours of irradiation for samples collected on May 23rd.

Compound	SML			ULW		
	Before irradiation	After 2.5 hours of irradiation	After 5 hours of irradiation	Before irradiation	After 2.5 hours of irradiation	After 5 hours of irradiation
Acetophenone	48	48	52	n.a.		
Acrolein	0	220	1098			
Benzaldehyde	6521	6596	7141			
Biacetyl	2017	3047	3385			
Butanal	58	187	381			
Crotonaldehyde	68	767	819			
Glyoxal	1882	2438	2693			
Heptanal	759	676	1139			
Hexanal	3365	3829	4448			
Isovaleraldehyde	1831	2322	2291			
Methacrolein	n.d.	251	468			
Methylglyoxal	749	1246	1602			
MVK	1278	1671	1992			
Octanal	81	73	138			
Propanal	1844	2691	3607			
Trans-2-hexenal	48	22	70			
Trans,trans-2,4-hexadienal	29	46	62			

n.d.: Not detectable; n.a.: Not available

65

Table S4: Concentrations of carbonyl compounds in nmol L^{-1} before, after 2.5 hours and after 5 hours of irradiation for samples collected on May 26th.

Compound	SML			ULW		
	Before irradiation	After 2.5 hours of irradiation	After 5 hours of irradiation	Before irradiation	After 2.5 hours of irradiation	After 5 hours of irradiation
Acetophenone	29	34	35	3	6	7
Acrolein	1139	4476	5811	n.d.	n.d.	314
Benzaldehyde	1071	1082	994	60	112	124
Biacetyl	1966	2830	3179	374	651	623
Butanal	n.d.	n.d.	n.d.	98	148	243
Crotonaldehyde	7398	8762	9158	423	466	590
Glyoxal	1006	1819	2355	912	1210	1127
Heptanal	885	596	1328	152	297	468
Hexanal	2178	3444	4823	551	915	1222
Isovaleraldehyde	11242	11528	11667	376	360	442
Methacrolein	2196	2813	3589	0	13	8
Methylglyoxal	677	1136	1337	274	441	419
MVK	2455	3323	6422	461	600	582
Octanal	n.d.	n.d.	28	n.d.	54	101
Propanal	n.d.	n.d.	n.d.	2940	3390	3675
Trans-2-hexenal	102	101	135	20	19	41
Trans,trans-2,4-hexadienal	3346	3369	3373	32	36	35

n.d.: Not detectable

70

Table S5: Concentrations of carbonyl compounds in nmol L^{-1} before, after 2.5 hours and after 5 hours of irradiation for samples collected on May 27th.

Compound	SML			ULW		
	Before irradiation	After 2.5 hours of irradiation	After 5 hours of irradiation	Before irradiation	After 2.5 hours of irradiation	After 5 hours of irradiation
Acetophenone	43	58	70	n.a.		
Acrolein	10539	10940	11986			
Benzaldehyde	4529	4369	4407			
Biacetyl	791	830	931			
Butanal	2172	4190	4379			
Crotonaldehyde	2132	2280	2349			
Glyoxal	2401	3060	2583			
Heptanal	5332	5340	5556			
Hexanal	26371	24528	25868			
Isovaleraldehyde	4597	4710	4808			
Methacrolein	30746	33997	54660			
Methylglyoxal	901	1123	1087			
MVK	27064	40011	62828			
Octanal	414	622	772			
Propanal	38117	39764	39613			
Trans-2-hexenal	700	624	755			
Trans,trans-2,4-hexadienal	3579	3551	3547			

n.a.: Not available

Table S6: Concentrations of carbonyl compounds in nmol L^{-1} before, after 2.5 hours and after 5 hours of irradiation for samples collected on May 28th.

Compound	SML			ULW		
	Before irradiation	After 2.5 hours of irradiation	After 5 hours of irradiation	Before irradiation	After 2.5 hours of irradiation	After 5 hours of irradiation
Acetophenone	37	69	66	6	6	9
Acrolein	2741	4379	5020	343	391	796
Benzaldehyde	4186	4186	3648	57	62	126
Biacetyl	2636	2910	3352	659	488	778
Butanal	1203	1351	1639	124	140	225
Crotonaldehyde	980	1251	1144	437	487	563
Glyoxal	10075	9215	11728	1648	1679	2155
Heptanal	2166	1846	1860	289	344	603
Hexanal	17643	12420	11485	1304	1642	2205
Isovaleraldehyde	2120	2396	1954	406	503	1093
Methacrolein	750	883	917	3	0	37
Methylglyoxal	2782	3042	3916	336	315	566
MVK	3038	3258	3832	568	581	1755
Octanal	520	326	274	91	60	29
Propanal	19417	20707	20767	5873	6038	7087
Trans-2-hexenal	428	447	505	46	53	123
Trans,trans-2,4-hexadienal	495	533	491	68	71	74

80

Table S7: Concentrations of carbonyl compounds in nmol L^{-1} before, after 2.5 hours and after 5 hours of irradiation for samples collected on May 30th.

Compound	SML			ULW		
	Before irradiation	After 2.5 hours of irradiation	After 5 hours of irradiation	Before irradiation	After 2.5 hours of irradiation	After 5 hours of irradiation
Acetophenone	165	182	191	1	1	3
Acrolein	34194	34244	46282	214	389	874
Benzaldehyde	4949	4283	4802	56	64	100
Biacetyl	5340	3482	7628	240	392	471
Butanal	14798	15284	20000	70	108	152
Crotonaldehyde	10273	12089	15561	n.d.	n.d.	n.d.
Glyoxal	17076	13880	22758	1748	1887	1655
Heptanal	8670	8138	10794	244	248	347
Hexanal	61443	51212	57762	850	1004	1239
Isovaleraldehyde	4338	4930	7051	327	254	250
Methacrolein	1016	2074	3542	0	0	0
Methylglyoxal	3135	3723	5139	355	369	298
MVK	13470	14955	20524	596	671	687
Octanal	802	446	627	22	50	77
Propanal	126758	129110	171869	4006	4524	5707
Trans-2-hexenal	3023	3003	2384	34	41	56
Trans,trans-2,4-hexadienal	1535	1476	1632	50	54	62

n.d.: Not detectable

Table S8: Concentrations of carbonyl compounds in nmol L^{-1} before, after 2.5 hours and after 5 hours of irradiation for samples collected on June 1st.

Compound	SML			ULW		
	Before irradiation	After 2.5 hours of irradiation	After 5 hours of irradiation	Before irradiation	After 2.5 hours of irradiation	After 5 hours of irradiation
Acetophenone	89	91	93	5	6	7
Acrolein	12372	22212	28659	3113	3643	4494
Benzaldehyde	4781	4647	4657	55	132	91
Biacetyl	1232	1377	1871	153	220	371
Butanal	17698	18342	18503	754	809	827
Crotonaldehyde	5634	6577	7468	1153	1302	1303
Glyoxal	7370	9382	12134	440	539	618
Heptanal	12721	16400	17580	735	882	995
Hexanal	89702	68921	65663	2209	2174	2174
Isovaleraldehyde	4811	4794	5817	406	750	659
Methacrolein	699	1497	1784	57	95	114
Methylglyoxal	2245	2853	3604	106	172	206
MVK	2800	3909	4545	1383	1545	1608
Octanal	2288	1988	2740	105	133	96
Propanal	130401	130580	128340	12512	12656	13044
Trans-2-hexenal	15772	15040	13508	145	138	154
Trans,trans-2,4-hexadienal	2766	2918	3036	74	77	75

Table S9: Concentrations of carbonyl compounds in nmol L^{-1} before, after 2.5 hours and after 5 hours of irradiation for samples collected on June 2nd.

Compound	SML			ULW		
	Before irradiation	After 2.5 hours of irradiation	After 5 hours of irradiation	Before irradiation	After 2.5 hours of irradiation	After 5 hours of irradiation
Acetophenone	35	44	24	2	6	7
Acrolein	7725	11415	11341	1507	1765	2728
Benzaldehyde	2646	2585	2577	38	87	143
Biacetyl	520	729	875	288	437	883
Butanal	6015	6682	5790	394	370	533
Crotonaldehyde	1862	2456	2650	617	212	668
Glyoxal	2981	2969	3830	749	1129	1921
Heptanal	3733	5916	7033	388	490	610
Hexanal	23202	20152	18397	2575	1985	2548
Isovaleraldehyde	4020	4300	3447	338	65	364
Methacrolein	872	1430	1163	0	0	54
Methylglyoxal	1345	1620	1921	250	424	810
MVK	1124	1329	1586	313	445	746
Octanal	787	590	795	91	98	140
Propanal	63719	66416	52173	8800	8148	9797
Trans-2-hexenal	3154	3190	2827	186	149	147
Trans,trans-2,4-hexadienal	809	810	858	88	97	129

Table S10: Concentrations of carbonyl compounds in nmol L^{-1} before, after 2.5 hours and after 5 hours of irradiation for samples collected on June 7th.

Compound	SML			ULW		
	Before irradiation	After 2.5 hours of irradiation	After 5 hours of irradiation	Before irradiation	After 2.5 hours of irradiation	After 5 hours of irradiation
Acetophenone	202	196	204	n.a.		
Acrolein	13649	20068	24867			
Benzaldehyde	10585	9610	9324			
Biacetyl	4124	3242	4607			
Butanal	7323	8037	9254			
Crotonaldehyde	1790	3223	3804			
Glyoxal	12073	14609	12331			
Heptanal	11997	10027	10716			
Hexanal	42701	36383	28242			
Isovaleraldehyde	19947	20210	19693			
Methacrolein	1158	1502	1756			
Methylglyoxal	4015	4764	5169			
MVK	1949	2756	2907			
Octanal	2441	2656	1605			
Propanal	80383	85070	91676			
Trans-2-hexenal	3987	4211	3134			
Trans,trans-2.4-hexadienal	2103	2328	2449			

n.a.: Not available

Table S11: Concentrations of carbonyl compounds in nmol L^{-1} before, after 2.5 hours and after 5 hours of irradiation for samples collected on June 8th.

Compound	SML			ULW		
	Before irradiation	After 2.5 hours of irradiation	After 5 hours of irradiation	Before irradiation	After 2.5 hours of irradiation	After 5 hours of irradiation
Acetophenone	52	119	153	17	29	36
Acrolein	8831	4630	8840	0	0	0
Benzaldehyde	1685	2313	2628	193	332	419
Biacetyl	896	1497	1693	238	311	372
Butanal	11982	5126	6419	34	107	162
Crotonaldehyde	n.d.	138	1139	1513	2042	2353
Glyoxal	3924	5798	5010	208	409	423
Heptanal	5069	3890	4083	179	0	31
Hexanal	24200	11313	11538	625	1357	1898
Isovaleraldehyde	267	1182	1553	421	554	651
Methacrolein	2333	0	0	3	7	11
Methylglyoxal	1360	2282	2264	108	168	254
MVK	5555	1638	1718	145	211	253
Octanal	585	926	689	173	402	539
Propanal	233871	49288	60243	77	320	472
Trans-2-hexenal	1934	659	780	n.d.	80	116
Trans,trans-2,4-hexadienal	447	985	1116	3	7	11

n.d.: Not detectable

Table S12: Concentrations of carbonyl compounds in nmol L^{-1} before, after 2.5 hours and after 5 hours of irradiation for samples collected on June 11th.

Compound	SML			ULW		
	Before irradiation	After 2.5 hours of irradiation	After 5 hours of irradiation	Before irradiation	After 2.5 hours of irradiation	After 5 hours of irradiation
Acetophenone	391	171	241	17	21	31
Acrolein	4234	5054	8222	0	0	0
Benzaldehyde	10239	4507	6056	292	287	430
Biacetyl	4485	3381	4227	384	446	345
Butanal	1821	1900	2685	184	307	599
Crotonaldehyde	0	0	0	0	0	0
Glyoxal	1814	2376	4213	996	941	1032
Heptanal	2460	1609	1146	0	437	392
Hexanal	11872	5818	8741	1203	1706	1686
Isovaleraldehyde	6496	4965	5607	n.d.	n.d.	n.d.
Methacrolein	529	273	606	n.d.	n.d.	n.d.
Methylglyoxal	1347	1531	2699	237	268	288
MVK	2635	2296	3113	1401	185	164
Octanal	950	322	855	160	273	234
Propanal	4163	3998	5948	692	1022	1016
Trans-2-hexenal	346	222	174	n.d.	95	9
Trans,trans-2,4-hexadienal	80	73	116	28	28	33

Table S13: Average standard error based on the different measured calibration levels.

Compound	Average standard error
Acetophenone	0.7 %
Acrolein	4.7 %
Benzaldehyde	5.1 %
Biacetyl	7.9 %
Butanal	0.6 %
Crotonaldehyde	1.3 %
Glyoxal	8.3 %
Heptanal	2.2 %
Hexanal	1.8 %
Isovaleraldehyde	2.3 %
Methacrolein	4.0 %
Methylglyoxal	7.9 %
MVK	2.1 %
Octanal	1.1 %
Propanal	3.6 %
Trans-2-hexenal	0.3 %
Trans, trans-2,4-hexadienal	0.7 %

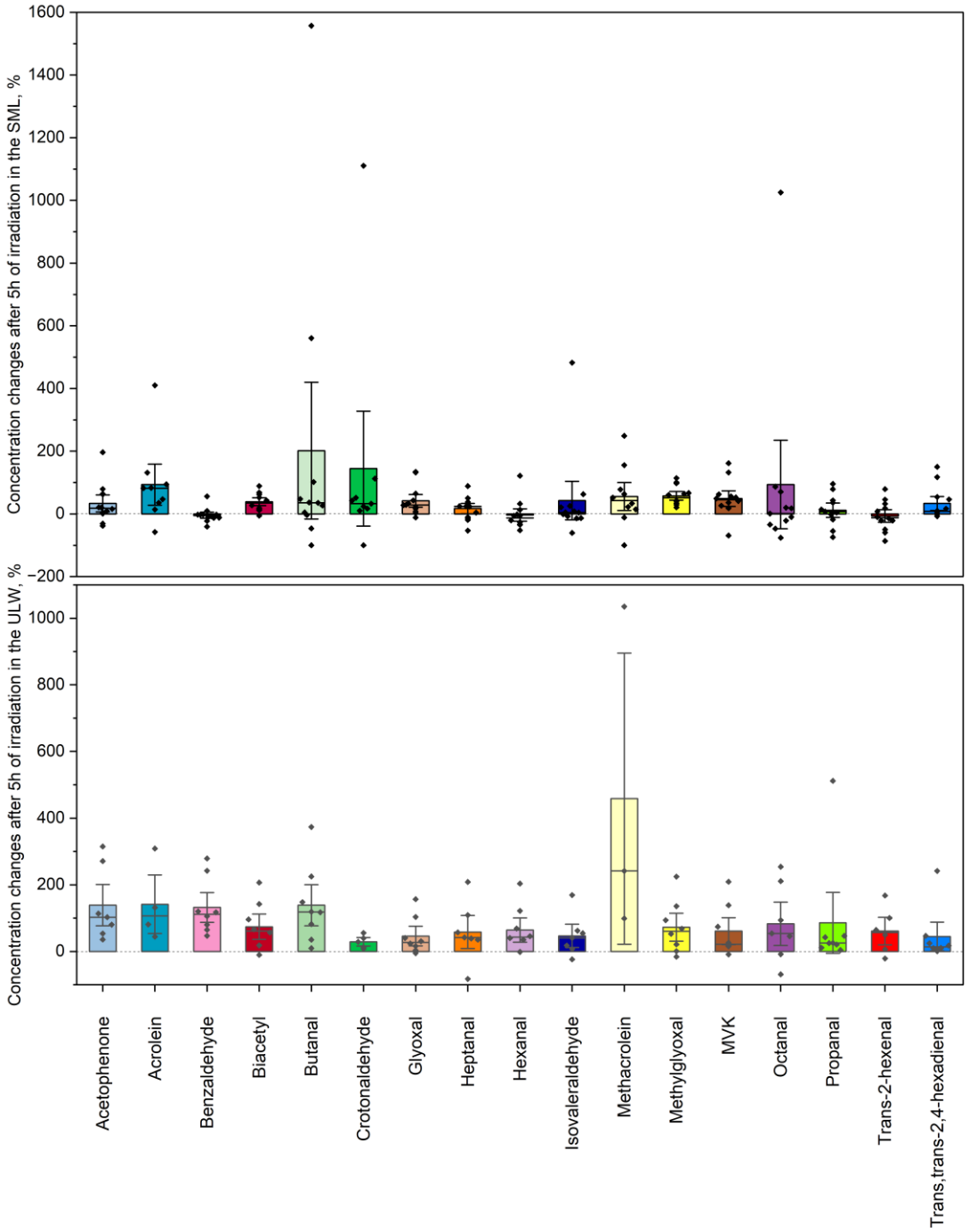

Figure S3: Relative concentration changes (%) after 5 hours of irradiation of 17 carbonyl compounds in the investigated SML and ULW samples. Boxes represent the interquartile range, the line in each box represents the median, and the whiskers extend to 1.5 times the interquartile range.

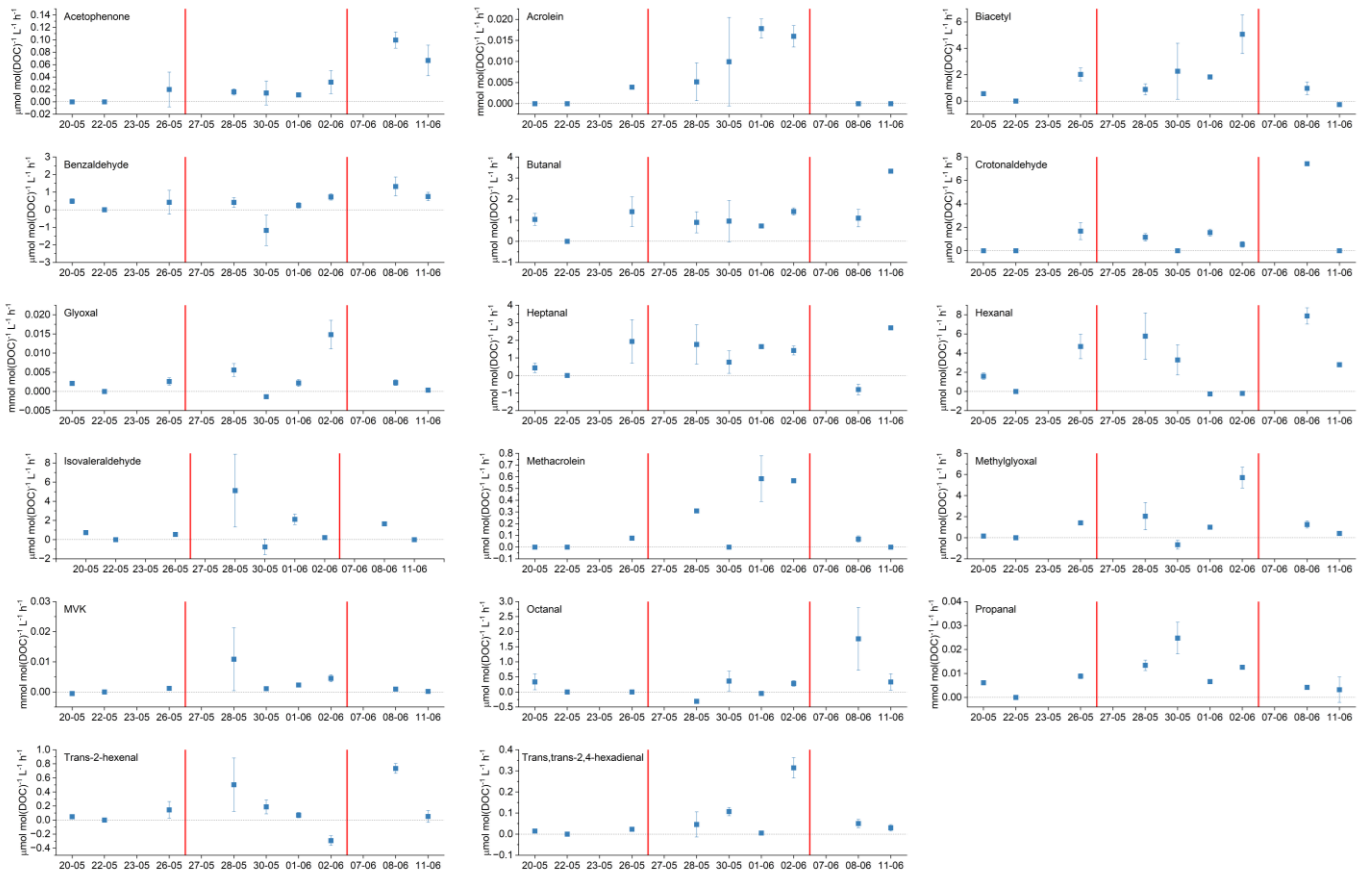

Figure S4: Photochemical production and degradation rates in the ULW samples on an expanded scale, including error bars that reflect analytical and sample-handling uncertainties.

S5 Estimated rates of transfer of carbonyl compounds from the SML to the gas interface

S5.1 Rates of transfer of photochemically-produced carbonyl compounds from the SML to the gas interface – Equilibrium partitioning

The compound-specific rates of transfer of carbonyl compounds from the liquid interface (c_{sl}) to the gas interface (c_{sg}) in all the samples under study were estimated using the two-layer model (Liss and Slater, 1974).

The already determined compound-specific formation rates in the SML (in M h^{-1}) were considered as the concentrations in the liquid interface (c_{sl}). The concentrations in the gas interface were then calculated with the following equation:

$$H = \frac{c_{sl}}{c_{sg}} \quad \text{(S4)}$$

Where H is the apparent partition coefficient (in M atm^{-1}). The resulting concentrations in the gas interface are converted from atm h^{-1} to M h^{-1} using the Ideal gas law:

$$c_{sg}, M\ h^{-1} = \frac{n}{V} = \frac{P}{R \times T} \quad \text{(S5)}$$

Where n is the number of moles (mol), V is the volume (L), P is the pressure (atm h^{-1}), R is the ideal gas constant (L atm mol^{-1} K^{-1}) and T is the temperature (K). A constant temperature of 298 K is assumed for all the calculations. Finally, the following equation was applied:

$$Rate\ of\ transfer\ to\ the\ gas\ interface = c_{sg}, M\ h^{-1} \times N_A \times SML\ thickness \quad \text{(S6)}$$

Where N_A is the Avogadro constant (6.022×10^{23} molecules mol^{-1}). A constant SML thickness of 100 μm is assumed for all the calculation. After the corresponding unit conversions, the final rates of transfer from the SML to the gas interface can be expressed in molecules cm^{-2} h^{-1}.

These steps were followed for all the samples investigated in both bloom and non-bloom conditions. The minimum and maximum values were used to define the estimated ranges (Table 2). Negative values were not considered for the ranges.

S5.2 Rates of transfer of glyoxal from the SML to the gas interface – Concentration gradient approach

A more realistic estimate using concentrations in both sides of the interface for glyoxal has been explored as a case-study. The transfer flux (F, nmol cm^{-2} s^{-1}) was calculated using Equation S7:

$$F = k \times \left(c_{sl} - \frac{c_{sg}}{H'}\right) \quad \text{(S7)}$$

For the concentrations in the water interface (c_{sl}), the measured minimum and maximum concentrations of glyoxal in bloom and non-bloom conditions for non-irradiated samples were considered. For the concentrations in the air interface (c_{sg}), the value of 10 ppt was used, as reported for the tropical Atlantic boundary layer (Walker et al., 2022). The standard gas transfer velocity (k, m s^{-1}) has been estimated as the product of the aqueous-phase diffusion coefficient of glyoxal (D, m^2 s^{-1}) and the thickness of the SML (100 µm). 1×10^{-9} m^2 s^{-1} was considered as the diffusion coefficient of glyoxal (Curry et al., 2018).

$$k = D \times SML\ thickness \quad \text{(S8)}$$

The resulting transfer fluxes range between $(1.7 – 20.8) \times 10^{-4}$ nmol cm^{-2} s^{-1} in non-bloom conditions, and $(4.1 – 29.4) \times 10^{-4}$ nmol cm^{-2} s^{-1}. In contrast to the rates of transfer of photochemically-produced carbonyl compounds from the SML to the gas interface calculated using equilibrium partitioning (Section S5.1), the transfer fluxes estimated using the concentration gradient approach consider total glyoxal concentrations measured in the non-irradiated SML and in the atmosphere in the marine environment. This means that the gradient-based transfer fluxes reflex overall values that integrate all possible processes, while the results obtained in Section S5.1 are limited to the photochemically-produced compounds.

S6 Calculation of apparent quantum yields (AQYs)

The apparent quantum yields (AQYs) were calculated following the approach of Zhang and Blough for polychromatic irradiations (Zhang and Blough, 2016):

$$AQY = \frac{R_{photo}}{R_{EX}} \quad \text{(S9)}$$

R_{photo} is the rate of photochemical formation or degradation of the investigated compound and R_{EX} is the rate of light excitation. REX has been calculated as the product of the wavelength-dependent lamp irradiance (I(λ), photons cm^{-2} s^{-1} nm^{-1}) and the Naperian absorption coefficient (α, cm^{-1}) for a spectral range of 280 nm to 550 nm.

$$R_{EX} = \int_{280}^{550} \alpha(\lambda) \times I(\lambda) d\lambda \quad \text{(S10)}$$

The Naperian absorption coefficient has been calculated using the absorbance of all the investigated samples (A) and the pathlength (l):

$$\alpha(\lambda) = 2.303 \times \frac{A}{l} \quad \text{(S11)}$$

R_{EX} was integrated using trapezoidal numerical integration.

The AQYs of the 17 carbonyl compounds for each investigated SML (red) and ULW (blue) samples are shown in Figure S3. In order to evaluate potential systematic relationships between the calculated photochemical efficiencies and the OM abundance, AQYs and DOC concentrations were compared (Figure S4).

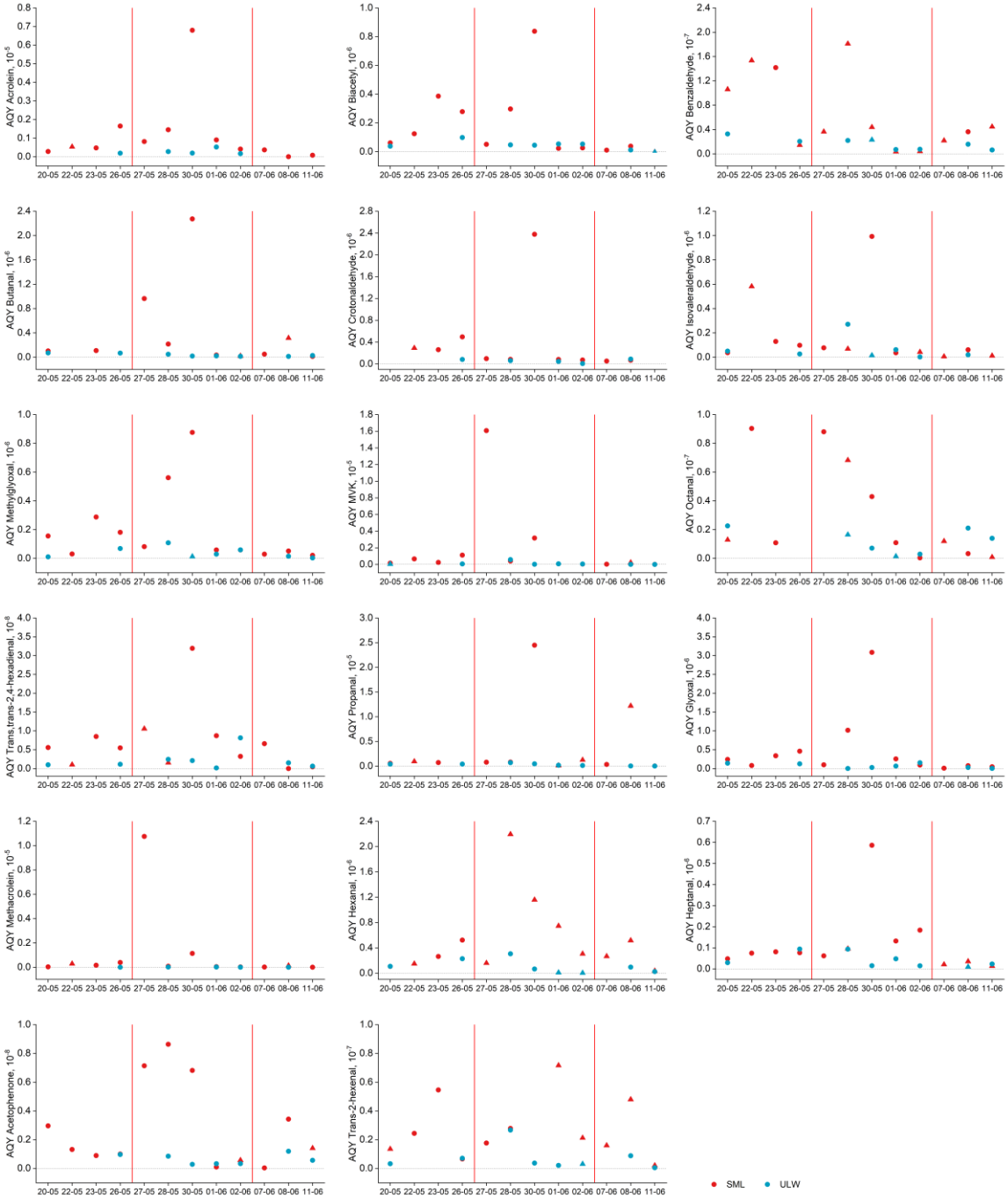

Figure S5: Calculated apparent quantum yields of the carbonyl compounds for each of the investigated SML (red) and ULW (blue) samples. Circles represent photochemical formation and triangles represent photochemical degradation.

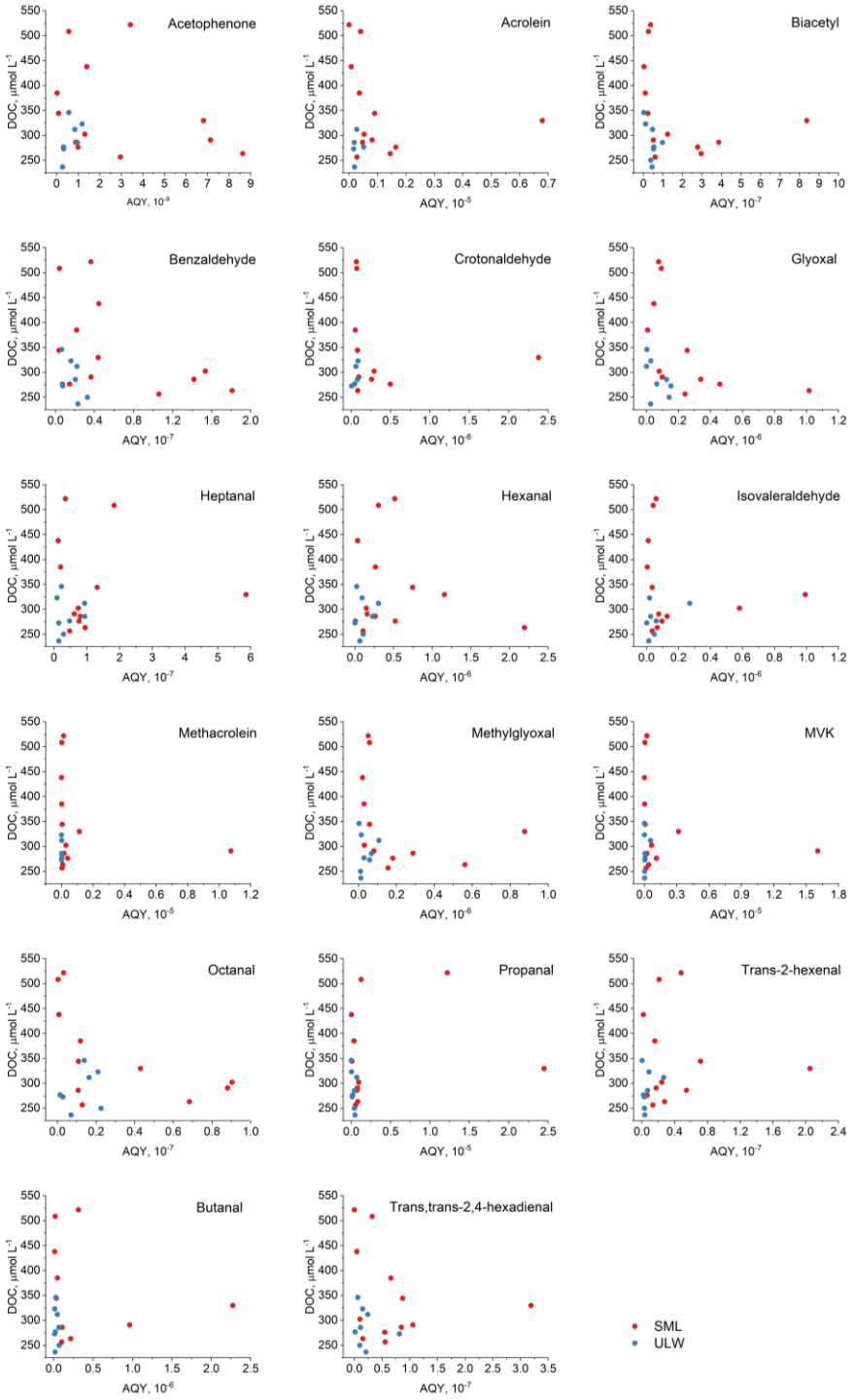

Figure S6: Calculated AQYs of the carbonyl compounds compared with the DOC concentrations.

215

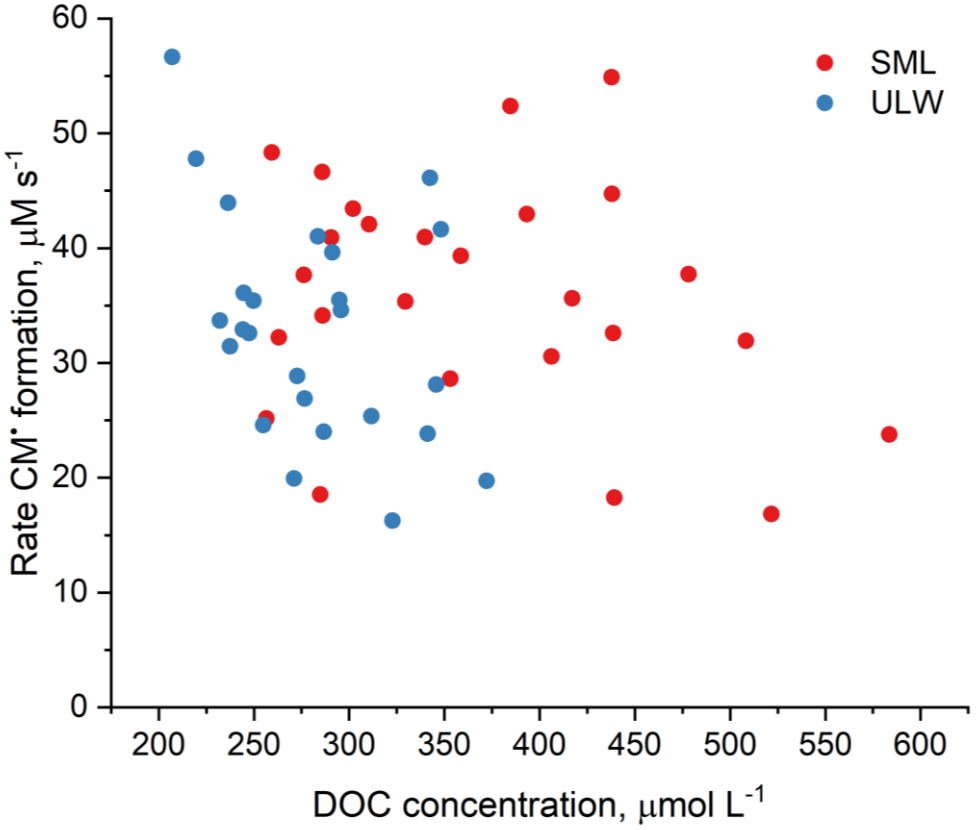

Figure S7: Calculated rates of CM radical formation compared with the DOC concentrations.

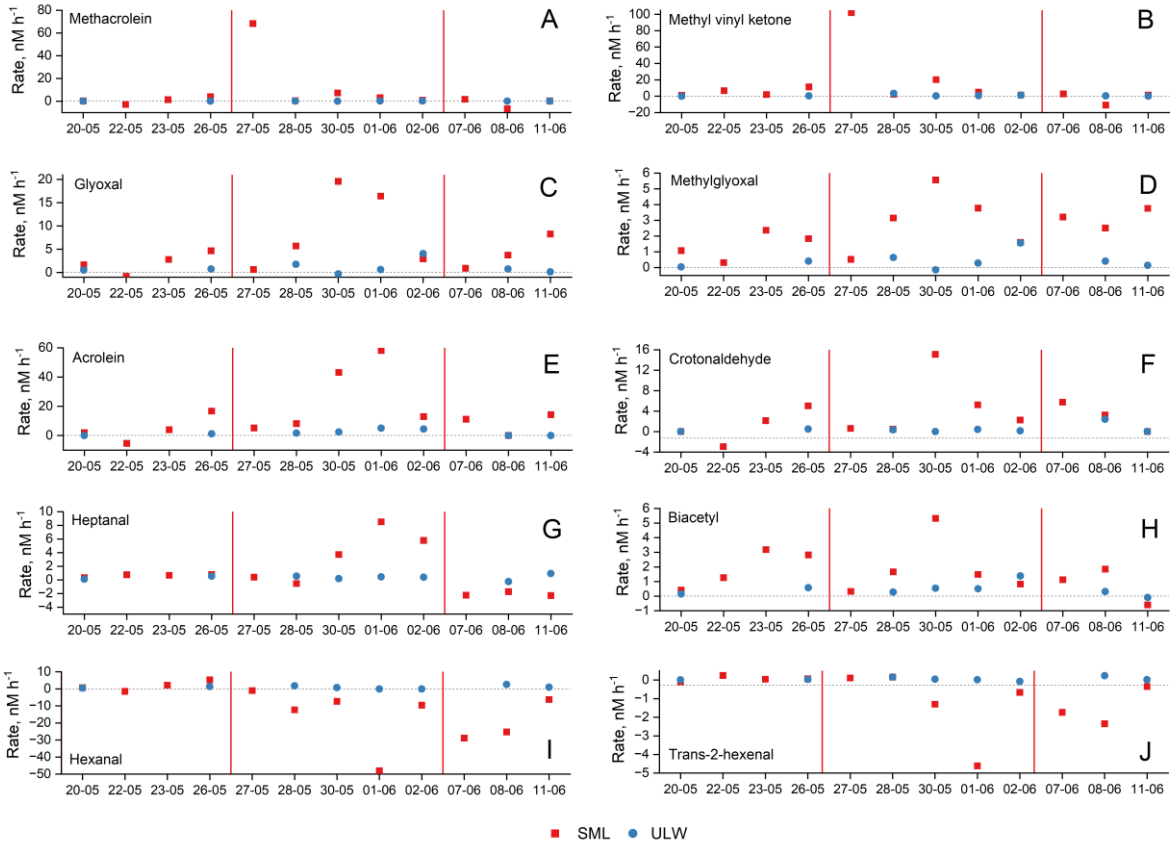

220 **Figure S8: Comparison of photochemical formation and degradation rates of methacrolein (A), MVK (B), glyoxal (C), methylglyoxal (D), acrolein (E), crotonaldehyde (F), heptanal (G), biacetyl (H), hexanal (I) and trans-2-hexenal (J) in the SML (red) and in ULW (blue). The red vertical lines separate the three phases of the mesocosm study: pre-bloom (20-05 to 26-05), bloom (27-05 to 02-06) and post-bloom (08-06 to 11-06).**

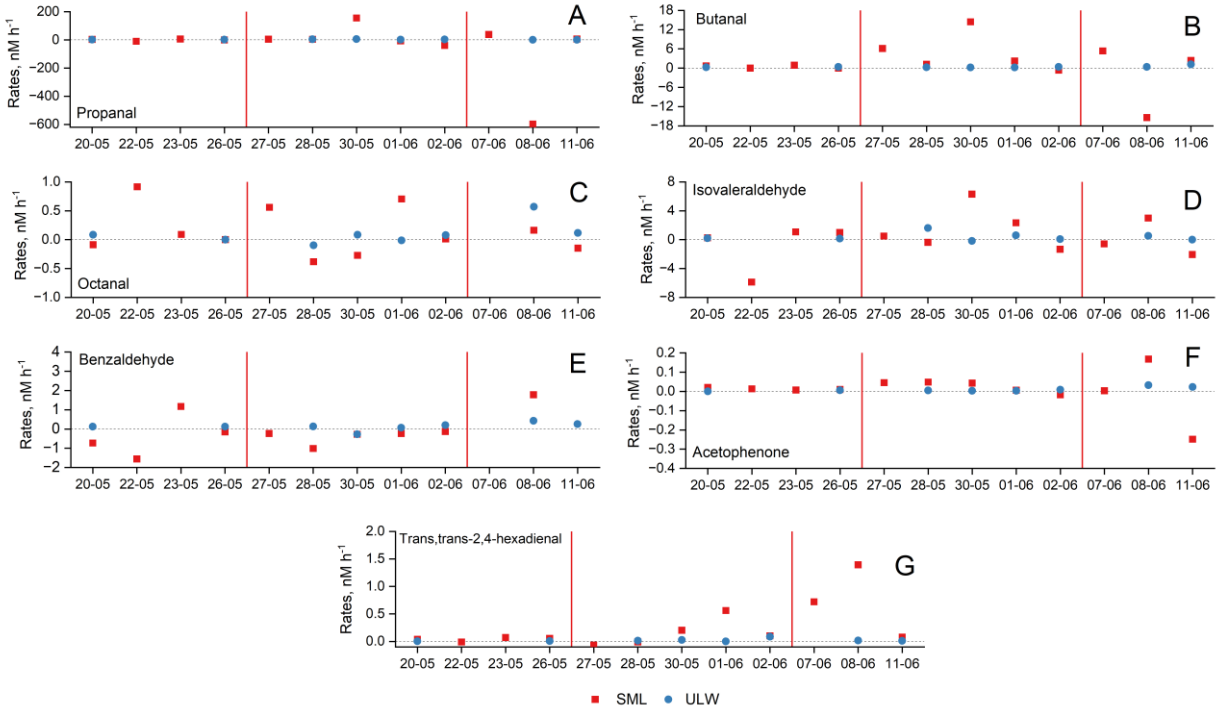

225

Figure S9: Comparison of photochemical formation and degradation rates of propanal (A), butanal (B), octanal (C), isovaleraldehyde (D), benzaldehyde (E), acetophenone (F) and trans,trans-2,4-hexadienal (G) in the SML (red) and in ULW (blue). The red lines separate the three phases of the mesocosm study: pre-bloom (20-05 to 26-05), bloom (27-05 to 02-06) and post-bloom (08-06 to 11-06).

230

S7 Relative changes in the contribution carbonyl compounds to non-purgeable organic carbon (NPOC) in unfiltered SML and ULW samples before and after irradiation

To assess changes in the contribution of carbonyls to DOC before and after 5 hours of irradiation, the changes in the relative contribution of the sum of C in the measured carbonyl compounds to non-purgeable organic carbon (NPOC) were quantified. NPOC was used as the closer operational proxy for DOC in selected, unfiltered SML and ULW samples before and after 5 hours of irradiation, one for each bloom phase. NPOC concentrations were measured using a TOC-VCPH analyser (Shimadzu, Japan). The obtained results are presented in Table S14.

Table S14: Relative changes in the contribution carbonyl compounds to NPOC in unfiltered SML and ULW samples, before irradiation and after 5 hours of irradiation.

Sample type	Date	Bloom phase	Contribution to NPOC before irradiation, %	Contribution to NPOC after irradiation, %	Changes in contribution to NPOC, %
SML	May 26th	Pre-bloom	0.21 %	0.22 %	0.01 %
SML	May 30th	Bloom	1.20 %	1.06 %	-0.14 %
SML	June 8th	Post-bloom	1.24 %	0.51 %	-0.73 %
ULW	May 23rd	Pre-bloom	0.05 %	0.18 %	0.13 %
ULW	May 30th	Bloom	0.11 %	0.16 %	0.05 %
ULW	June 8th	Post-bloom	0.04 %	0.10 %	0.06 %

The relative contribution of carbonyl compounds to NPOC was always below 1 % and did not increase considerably after irradiation. For the SML, relative changes indicate no net accumulation and suggest rapid photochemical turnover. Changes in ULW were smaller and more uniform, with suggest a limited net accumulation. The obtained results demonstrate that irradiation does not result in a significant enrichment of carbonyl compounds relative to the OC concentrations and indicate that OC abundance alone is not sufficient to explain differences in photochemical rates. This is in agreement with the AQY analysis and the trends in the normalized photochemical rates.

References

Curry, L. A., Tsui, W. G., and McNeill, V. F.: Technical note: Updated parameterization of the reactive uptake of glyoxal and methylglyoxal by atmospheric aerosols and cloud droplets, Atmos. Chem. Phys., 18, 9823-9830, doi: 10.5194/acp-18-9823-2018, 2018.

Demas, J. N., Bowman, W. D., Zalewski, E. F., and Velapoldi, R. A.: Determination of the quantum yield of the ferrioxalate actinometer with electrically calibrated radiometers, J. Phys. Chem., 85, 2766-2771, doi: 10.1021/j150619a015, 1981.

Goldstein, S. and Rabani, J.: The ferrioxalate and iodide-iodate actinometers in the UV region, J. Photoch. Photobio. A, 193, 50-55, doi: 10.1016/j.jphotochem.2007.06.006, 2008.

Hatchard, C. G. and Parker, C. A.: A New Sensitive Chemical Actinometer. II. Potassium Ferrioxalate as a Standard Chemical Actinometer, Proc. R. Soc. Lon. A Math. Phys. Sci., 235, 518-536, doi: 10.1098/rspa.1956.0102, 1956.

Langford, C. H. and Holubov, C. A.: Wavelength and temperature dependence in the photolysis of the chemical actinometer, potassium trisoxalatoferrate(III), at longer wavelengths, Inorg. Chim. Acta, 53, L59-L60, doi: 10.1016/S0020-1693(00)84742-8, 1981.

Lee, J. and Seliger, H. H.: Quantum Yield of Ferrioxalate Actinometer, J. Chem. Phys., 40, 519-523, doi: 10.1063/1.1725147, 1964.

Liss, P. S. and Slater, P. G.: Flux of Gases Across Air-Sea Interface, Nature, 247, 181-184, doi: 10.1038/247181a0, 1974.

Walker, H., Stone, D., Ingham, T., Hackenberg, S., Cryer, D., Punjabi, S., Read, K., Lee, J., Whalley, L., Spracklen, D., Carpenter, L. J., Arnold, S. R., and Heard, D. E.: Observations and modelling of glyoxal in the tropical Atlantic marine boundary layer, Atmos. Chem. Phys., 22, 5535-5557, doi: 10.5194/acp-22-5535-2022, 2022.

Wegner, E. E. and Adamson, A. W.: Photochemistry of Complex Ions .III. Absolute Quantum Yields for Photolysis of Some Aqueous Chromium(III) Complexes. Chemical Actinometry in Long Wavelength Visible Region, J. Am. Chem. Soc., 88, 394-404, doi: 10.1021/ja00955a003, 1966.

Zhang, Y. and Blough, N. V.: Photoproduction of One-Electron Reducing Intermediates by Chromophoric Dissolved Organic Matter (CDOM): Relation to O_2^- and H_2O_2 Photoproduction and CDOM Photooxidation, Environ. Sci. Technol., 50, 11008-11015, doi: 10.1021/acs.est.6b02919, 2016.